Chemical Science

ROYAL SOCIETY OF CHEMISTRY

EDGE ARTICLE

View Article Online
View Journal | View Issue

Cite this: *Chem. Sci.*, 2021, **12**, 12719

All publication charges for this article have been paid for by the Royal Society of Chemistry

Received 25th April 2021
Accepted 18th August 2021

DOI: 10.1039/d1sc02302k

rsc.li/chemical-science

Sulfated poly-amido-saccharides (sulPASs) are anticoagulants *in vitro* and *in vivo*†

Maria Varghese, [a] Rae S. Rokosh, [b] Carolyn A. Haller, [b] Stacy L. Chin,[a] Jiaxuan Chen, [b] Erbin Dai,[b] Ruiqing Xiao, [a] Elliot L. Chaikof *[b] and Mark W. Grinstaff *[a]

Anticoagulant therapeutics are a mainstay of modern surgery and of clotting disorder management such as venous thrombosis, yet performance and supply limitations exist for the most widely used agent – heparin. Herein we report the first synthesis, characterization, and performance of sulfated poly-amido-saccharides (sulPASs) as heparin mimetics. sulPASs inhibit the intrinsic pathway of coagulation, specifically FXa and FXIa, as revealed by *ex vivo* human plasma clotting assays and serine protease inhibition assays. sulPASs activity positively correlates with molecular weight and degree of sulfation. Importantly, sulPASs are not degraded by heparanases and are non-hemolytic. In addition, their activity is reversed by protamine sulfate, unlike small molecule anticoagulants. In an *in vivo* murine model, sulPASs extend clotting time in a dose dependent manner with bleeding risk comparable to heparin. These findings support continued development of synthetic anticoagulants to address the clinical risks and shortages associated with heparin.

Introduction

Anticoagulants control, prevent, and treat clotting disorders, and are routinely used in surgery for the treatment of thromboembolic disorders.[1,2] Unfractionated heparin (UFH), a sulfated glycosaminoglycan extracted from porcine mucosa, is the most widely used anticoagulant.[3,4] Today, there is an imminent risk of a global shortage of heparin due to the current epidemic of African Swine Fever.[5,6] This virus has wiped out over one-quarter of the world's pig population.[7] In 2008, a similar porcine ailment in China resulted in global shortages and in emergence of adulterated UFH and low molecular weight heparin (LMWH), leading to patient deaths.[8,9]

Heparin is primarily used for thromboprophylaxis to prevent venous or arterial thrombus (*i.e.*, clot) formation due to cancer, thrombophilia, or immobility.[10] Prophylactic use of LMWH, prepared by chemical or enzymatic degradation of unfractionated heparin[11] prevents the occurrence of deep vein thrombosis and pulmonary embolism,[12] one of the most prevalent, but preventable, causes of death in hospitalized patients. Unlike UFH, which requires diligent monitoring due to its highly variable activity[13] and patient-dependent dose-responses,[11,14,15] LMWH displays less variability in its bioactivity, as well as higher bioavailability.[16] In spite of its advantages and widespread use, LMWH, similar to UFH leads to heparin induced thrombocytopenia (HIT)[17–19] in 1–5% of patients,[20] and its anticoagulant effect is only partially neutralized using protamine sulfate.[21] All told, the development of synthetic heparin alternatives is of keen interest and of clinical importance.

Fondaparinux is a synthetic penta-saccharide consisting of the minimal antithrombin binding region of heparin.[22] While fondaparinux is not associated with HIT,[23] unlike UFH or LMWH, it cannot be effectively reversed, which, along with its high plasma half-life of ≈19 hours is associated with an increased bleeding risk.[24] The synthesis of fondaparinux is a multi-step (20+) procedure requiring protected monosaccharides and precise control of stereo orientation during the glycosylation reactions.[22,25] A variety of sulfated polymers[26] have been explored as heparin substitutes, including linear polymers of sulfated dextran[27] and fucosylated chondroitin sulfate.[28] Promising *in vivo* activity has been observed but the ability to rapidly and reliably reverse the anticoagulant activity of these polymers has not been reported. Completely synthetic mimetics are less well studied and include polymers comprised of a non-carbohydrate backbone with pendant sulfated sugars[29–32] and branched sulfated polyglycerols.[33] These sulfated polymers possess limited *in vitro* anticoagulant activity as compared to UFH and few are reversed by protamine sulfate. Moreover, *in vivo* studies are very rarely reported.

[a]*Departments of Chemistry, Biomedical Engineering, and Medicine, Boston University, Boston, MA 02215, USA. E-mail: mgrin@bu.edu; mariavar@bu.edu; stacy.chin@hydroglydecoatings.com; xiaorq@mit.edu*

[b]*Department of Surgery, Beth Israel Deaconess Medical Center, Harvard Medical School, Wyss Institute of Biologically Inspired Engineering of Harvard University, Boston, MA, USA. E-mail: echaikof@bidmc.harvard.edu; rsrokosh@bidmc.harvard.edu; challer@bidmc.harvard.edu; jchen13@bidmc.harvard.edu; edai@bidmc.harvard.edu; mailto:echaikof@bidmc.harvard.edu*

† Electronic supplementary information (ESI) available. See DOI: 10.1039/d1sc02302k

Given the biological activity of heparin arises from electrostatic and hydrogen bond interactions between the sulfate groups on a rigid carbohydrate backbone and antithrombin III,[34,35] we envision that a synthetic polymer that structurally and functionally mimics heparin will provide insights into the design and applications of new polymeric anticoagulants, with the ultimate goal of a reversible, heparanase resistant agent with higher potency and greater selectivity of action to maximize therapeutic benefits while mitigating associated risks. Herein, we report the first synthesis and characterization of a heparin-mimetic, sulfated glucose-derived poly-amidosaccharide (sulPAS; Fig. 1). PASs are enantiopure polymers composed of sugar units connected by an α-1,2-amide peptide[36] linkage as opposed to an ether linkage[37] and possess a linear helical conformation.[38–42] Further we evaluate the anticoagulant activity using *in vitro* serine protease inhibition assays, *ex vivo* human plasma clotting assays, and an *in vivo* murine bleeding model. sulPAS anticoagulant activity depends upon the degree of sulfation and chain length, and is reversed by treatment with protamine sulfate.

Results and discussion

Synthesis and chemical characterization of sulPASs

We synthesized a library of PAS derivatives by anionic ring opening polymerization (AROP) of a glucose derived β-lactam monomer[38] with *t*-butyl benzoyl chloride as the initiator. Reduction of the benzyl-protected polymers followed by dialysis purification and lyophilization afforded the desired product (Fig. 1 and Table 1). Similarly, we prepared a galactose PAS (galPAS, DP = 12). Estimation of the molecular weight by ^{1}H NMR spectroscopy for gluPAS-12 and galPAS-12 agreed with GPC data (Fig. S1 and S4†).

We explored several sulfation strategies to synthesize the sulPAS post polymerization, including the use of different sulfation reagents, such as $SO_3 \cdot NMe_3$, $SO_3 \cdot DMF$, $SO_3 \cdot EtOH$, $SO_3 \cdot$pyridine, pyridine/$HClSO_3$; solvents such as DMF, pyridine or DMSO; reaction times ranging from 5 hours to 7 days; and temperatures from 25–70 °C. Based on the results of this screen, we dissolved PASs in anhydrous DMF and added 3 eq. or 5 eq. of $SO_3 \cdot NMe_3$ to the reaction mixture followed by stirring at 50 °C for 5 days (Fig. 1C),[43] to access low sulfated PAS (sulPAS-LS) or high sulfated PAS (sulPAS-HS), respectively. We quenched the reaction with NaOH, filtered it through a 0.4 μm syringe filter,

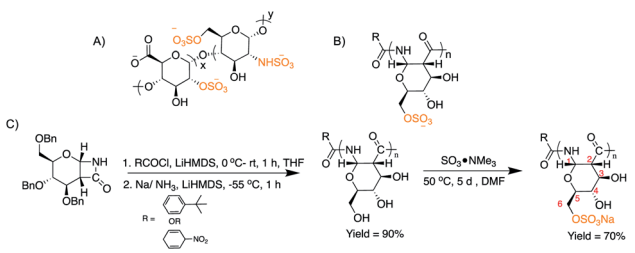

Fig. 1 (A) Structure of heparin; (B) structure of sulPAS; (C) synthetic scheme of sulPAS.

Table 1 GPC characterization and elemental analysis (E.A.) results of sulPAS and gluPAS samples

	PAS		sulPAS			
Sample	M_n[a] (kDa)	$Đ$	M_n[a] (kDa)	$Đ$	DS[b]	IU mg^{-1}[c]
Glu-12	2.0	1.2	2.4	1.2	1.0 (LS)	3.15 ± 0.5
Glu-12	2.0	1.2	4.6	1.2	1.9 (HS)	5.03 ± 1.1
Glu-25	3.0	1.3	9.2	1.4	1.3 (HS)	6.79 ± 3.0
Glu-50	4.1	1.4	14.2	1.4	1.4 (HS)	6.96 ± 1.8
Gal-12	2.6	1.1	4.24	1.2	1.6 (HS)	2.91 ± 0.7

[a] GPC analyses were conducted in aqueous buffer *versus* dextran standards. [b] Elemental analyses were conducted to estimate DS. [c] IU mg^{-1} was calculated from APTT assay.

and removed the residual trimethyl amine by high-vacuum prior to neutralization with HCl, dialysis against distilled water for 24 hours and subsequent lyophilization. Following this procedure, we also prepared a galactose sulPAS (DP = 12) starting from galactose PAS (Table 1). sulPASs are water-soluble white powders with degrees of sulfation (DS; average number of sulfate groups per monomer; calculated from elemental analysis; Table 1) from 1 to 1.9. Symmetric $(S{=}O)_2$ and S–O–C stretching bands at ~1200 cm^{-1} and in the range 1000–769 cm^{-1}, respectively, are present in the IR spectrum of sulPAS indicative of *O*-sulfation (Fig. S15 and S16†). From the cross-peaks in the HSQCAD spectrum, the shift of methylene C^6 position in glu-sulPAS (which are distinct in HSQCAD from methine C^3, C^4 and C^5) as compared to gluPAS is consistent with C^6 sulfation (Fig. S10–S14†). However, ascertaining the next position of sulfation in polymers with DS > 1 was not possible because of the difficulty of assigning multiple new cross-peaks in the spectra. The sulPAS displays a prominent peak shift to earlier retention times (Fig. S17†) in aqueous GPC characterization due to an increase in the molecular weight (MW) and anionic charges on the sulPAS structure in contrast to the neutral gluPAS samples.[44] Circular dichroism (CD) spectra of glu-12-LS and glu-12-HS show a maxima at 186 nm and minima at 220 nm (Fig. S18†), consistent with the sulPASs adopting an α-helical secondary structure in aqueous environments similar to PASs.

In vitro anticoagulant activity of sulPASs

We first determined the activated partial thromboplastin time (APTT) and prothrombin time (PT) for sulPAS in human plasma as a measure of compound inhibition of the intrinsic and extrinsic pathways of the coagulation system, respectively (see Fig. S19† for the coagulation cascade).[45] Varying concentrations of sulPAS, heparin, or fondaparinux were added to normal human plasma (NHP), and we measured the clotting times[46] (Fig. 2A). Heparin (1 IU mL^{-1}) increases both APTT and PT as compared to the HEPES buffered saline (HBS) control; effecting both intrinsic and extrinsic pathways (Fig. 2). In contrast, the sulPAS only increases APTT, but not PT (Fig. 2), indicating selective inhibition of the intrinsic pathway of coagulation. The graph is also plotted with polymer concentration expressed in

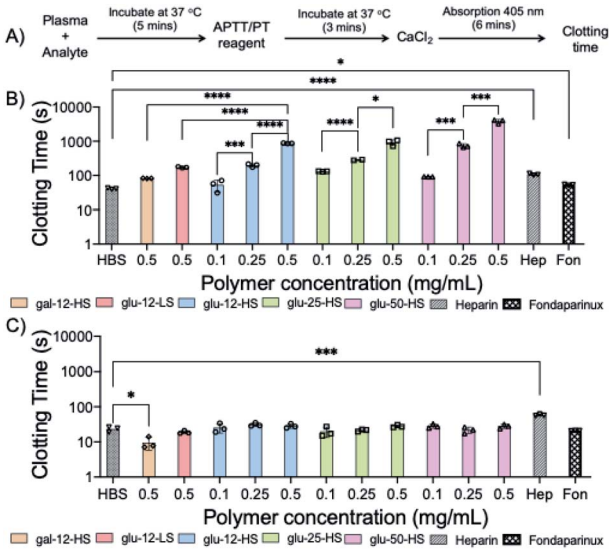

Fig. 2 (A) Schematics of *ex vivo* APTT and PT assay protocol in normal human plasma; (B) APTT increases with increase in concentration, chain length and degree of sulfation; (C) no statistically significant change in PT compared to HBS was observed with increase in concentration, chain length and concentration. Data represent mean ± SD, $n = 3$, $^{*}P \leq 0.05$, $^{***}P \leq 0.001$, $^{****}P \leq 0.0001$ (*post hoc* Student's *t*-test). Concentration of heparin control used is 1 IU mL^{-1}. Concentration of fondaparinux is 1 μg mL^{-1}. There was no significant difference observed from HBS for all data points in (C) except the ones that are represented.

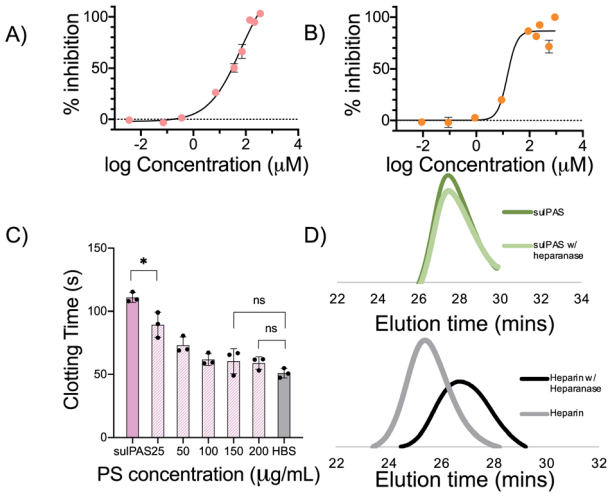

Fig. 3 (A) glu-50-HS inhibits FXa with an IC_{50} of 64.7 μM. (B) glu-50-HS inhibits FXIa with an IC_{50} of 14.58 μM. (C) Statistically significant difference in APTT of 100 μg mL^{-1} glu-50-HS is observed with the addition of 25 μg mL^{-1} protamine sulfate (PS). No significant difference in APTT with respect to HBS was observed with 100 μg mL^{-1} PS. (D) Representative elution profile of unfractionated heparin and glu-25-HS in the presence and absence of heparanase. a, b and c data represent mean ± SD, $n = 3$, $^{*}P \leq 0.05$ (unpaired Student's *t*-test).

IU mL^{-1} to aid in the analysis of activity (Fig. S20†). The pentasaccharide fondaparinux (1 μg mL^{-1}) also selectively increases APTT and not PT. Importantly, the non-sulfated PAS controls does not affect APTT or PT (Fig. S21†). APTT increases with greater sulPAS chain length and degree of sulfation. Additionally, the longer clotting time for the glucose-based PAS, compared to the galactose-based PAS, suggests that the anticoagulant activity of sulPAS depends on the spatial orientation of the sulfate group. Finally, we estimated the anticoagulant activity of the polymers in IU mg^{-1} using a standard curve of APTT *versus* heparin concentration (Fig. S22†).

To further investigate the mechanism of action, we assessed the antithrombin-III (AT-III) dependent inhibition of amidolytic activity of factor Xa (FXa) and thrombin in the presence of sulPAS (see ESI† for assay procedure). FXa and thrombin are downstream in the coagulation cascade and heparin (180 IU mg^{-1}, MW = 15 kDa) inhibits these enzymes with an IC_{50} of 0.02 μM (Fig. S23†) and 0.04 μM (Fig. S24†), respectively. The sulPAS with greatest anticoagulant activity according to APTT, glu-50-HS (6.96 ± 1.8 IU mg^{-1}) exhibits an IC_{50} of 64.7 μM for FXa (Fig. 3A), whereas thrombin inhibition by sulPAS shows an ascending limb, pseudo plateau and a descending limb, indicative of a template mechanism of inhibition[47] with optimal concentration for maximal inhibition ~30.3 μM (Fig. S24†). We also studied the inhibition of amidolytic activity of FXa and thrombin by glu-50-HS in the absence of AT-III (Fig. S25 and S26,† respectively). glu-50-HS does not inhibit FXa in the absence of AT-III, even at high concentrations (up to 3.57 mM, Fig. S25†), thus confirming the requirement of AT-III for FXa inhibition by sulPASs. On the other hand, thrombin inhibition exhibits an ascending limb, pseudo plateau and a descending limb, in the absence of AT-III (Fig. S26†), as is observed in the presence of AT-III. The percent maximum inhibition of thrombin by glu-50-HS is higher in the presence of AT-III (~57% *vs.* ~40% in the absence of AT-III). This result suggest glu-50-HS follows a template mechanism for inhibition of thrombin in the presence and absence of AT-III, with the presence of AT-III slightly improving the percent maximum inhibition.

These relatively high IC_{50} values of FXa and thrombin are inconsistent with the prolonged APTT, suggesting that other proteases in the intrinsic pathway are involved in the anticoagulant effect of sulPAS. Therefore, we examined the inhibitory effect of sulPAS on FXIa and FXIIa – two serine proteases in the intrinsic pathway, unaffected by heparin, identified as potential novel anticoagulant targets.[48–50] glu-50-HS inhibits FXIa with an IC50 of 14.58 μM (Fig. 3B). This result is similar to the FXIa inhibition effect of dextran sulfate reported by Hack *et al.*[51] The sulPAS does not inhibit FXIIa at lower concentrations and moderately activates the enzyme at high concentrations (Fig. S28†). We propose that the anticoagulant activity of sulPAS, observed in APTT assay, arises primarily from inhibition of FXIa, along with a modest inhibitory effect on FXa and thrombin.

Elevated plasma levels of heparanases, observed in patients with diabetes and renal insufficiency, may contribute to variable bioactivity.[52] Hence, we evaluated the susceptibility of sulPAS to heparanase degradation. Heparanase degrades unfractionated heparin but not sulPAS as determined by size-exclusion chromatography SEC (Fig. 3D). Given the molecular weight of the sulPAS, we propose that the sulPAS polymer will be cleared by

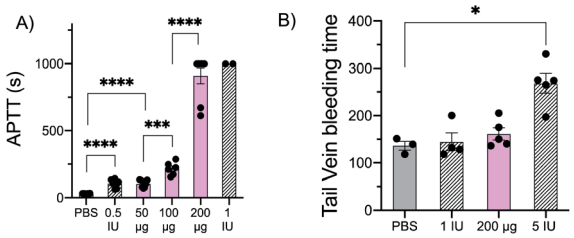

Fig. 4 (A) PBS, heparin (0.5 IU, 1.0 IU), or glu-50-HS (50–200 µg) were administered (IV) to C57BL/6 mice 3 minutes prior to blood draw, and plasma clotting time was measured on a microcoagulometer. glu-50-HS demonstrated a dose dependent increase in APTT. (B) Tail vein transection was performed 3 min post IV administration; significant prolongation of bleeding time was only observed after administration of positive control (5 IU heparin). Data represent mean ± SEM, $n = 3$–6 mice per agent, $*P \leq 0.05$, $***P \leq 0.001$, $****P \leq 0.0001$ (ANOVA and *post hoc* Student's *t*-test).

the kidneys, as the glomerular filtration cut-off is 50–60 kDa.[53] However, this will need to be experimentally determined *via* a radiolabeled pharmacokinetics and biodistribution study.

One of the concerns pertaining to the use of LMWH and fondaparinux is the lack of reversal agents. Thus, we investigated the ability of protamine sulfate (PS), a cationic polypeptide that clinically reverses unfractionated heparin, to inhibit sulPAS' anticoagulant activity. We added varying concentrations (25–200 µg mL^{-1}) of PS to a solution of NHP and 100 µg mL^{-1} of glu-50-HS and measured APTT. The prolonged clotting time of NHP with sulPAS shortens with the addition of 25 µg mL^{-1} PS and normalizes (*i.e.*, not statistically significant from HBS control) with the addition of 150 µg mL^{-1} of PS (Fig. 3C). A similar assay using 1 IU mL^{-1} UFH shows a statistically significant decrease in APTT with 25 µg mL^{-1} of PS (Fig. S29†).[54]

We also evaluated the cytotoxicity of sulPAS in comparison with UFH, gluPAS, and dextran using a standard MTS colorimetric assay. NIH 3T3 fibroblast mammalian cells were incubated in the presence of these reagents at varying concentrations ranging from 1.0 to 0.05 mg mL^{-1} for 24 hours. All samples display minimal cytotoxicity with results comparable to media control, particularly at low concentrations. However, sulPASs are slightly more cytotoxic at high concentration of 1.0 mg mL^{-1} (Fig. S30†).

We subsequently evaluated the hemolytic activity of sulPAS by incubating the polymers with human red blood cells (RBCs) at varying concentrations (0.125–1 mg mL^{-1}) of glu-50-HS and unfractionated heparin at 37 °C for 24 hours. Heparin and glu-50-HS show only a minimal hemolytic effect (Fig. S31†).

In vivo anticoagulant activity of sulPASs

Given these *in vitro* results, we evaluated the performance of glu-50-HS *in vivo*. Intravenous administration of glu-50-HS at doses ranging from 50 µg to 200 µg in a mouse affords a dose dependent increase in APTT (Fig. 4A), consistent with the *ex vivo* dose-dependent anticoagulant effect of glu-50-HS. We next determined the effect of glu-50-HS on hemostasis in a mouse tail vein transection bleeding time assay. glu-50-HS (200 µg) and low dose heparin (1 IU) did not significantly prolong bleeding time in comparison to saline vehicle (Fig. 4B). These results suggest that sulPAS can be dosed to achieve a clinically relevant increase in APTT with comparable bleeding risk to heparin.

Conclusions

In summary we describe the synthesis of heparin mimicking sulPASs. sulPAS anticoagulant activity positively correlates with molecular weight and degree of sulfation. Mechanistically, sulPASs inhibit the amidolytic activity of FXa and FXIa, with minimal effect on thrombin and FXIIa. sulPAS are not susceptible to heparanase degradation and their anticoagulant activity is reversed by protamine sulfate. When administered *in vivo*, sulPASs demonstrate a dose dependent increase in clotting time. The current limitations of animal derived heparin warrant the development of novel heparin analogs to include bioengineered analogs,[55,56] small molecule agents,[22] and polymer anticoagulant therapeutics.

Experimental

Synthetic procedure

gluPAS ($n = 12$, 25 and 50) and galPAS ($n = 12$) were prepared as previously described.[39,57]

General procedure for polymerization. To synthesize 12 mer, 3,4,6-tri-*O*-benzyl-D-glucose lactam (1.08 g, 2.34 mmol) was dissolved in 20 mL of distilled tetrahydrofuran (THF). 4-*tert*-Butylbenzoyl chloride or 4-nitrobenzoyl chloride (0.19 mmol, 1/12 eq. for 12 mer) in THF (0.10 mL) was added and the reaction flask was cooled to 0 °C. Next, LiHMDS in THF (81.5 mg, 0.49 mmol) was added and the solution was stirred at room temperature for 1 hour, after which, a pipette of saturated NH_4Cl solution was added. THF was removed and the resulting solid was redissolved in diethyl ether (50 mL) and washed with 1 M HCl, saturated $NaHCO_3$, and brine. After drying over sodium sulfate, the crude polymer was isolated by evaporation of solvent and then redissolved in minimum amount of dichloromethane. The polymer was precipitated by dropwise addition into a flask with stirred, cold pentane, and then collected by filtration. After drying under high vacuum, 0.96 g (88%) of an amorphous solid was isolated. A similar procedure was followed with variations in initiator (0.04 mmol for 25 mer and 0.02 mmol for 50 mer) and LiHMDS (0.1 mmol for 25 mer and 0.05 mmol for 50 mer) to synthesize PASs of varying chain-lengths. 3,4,6-Tri-*O*-benzyl-D-galactose lactam was used to synthesize the galPAS. ^{1}H NMR and GPC data matched those previously reported.

General procedure for debenzylation. Liquid ammonia was condensed into a three-necked round bottom flask, maintained at −62 °C (chloroform/dry ice cooling bath). Small pieces of sodium metal were added, at which point the solution turned blue. Next, 0.96 g (2.08 mmol) of gluPAS'-12, dissolved in 5 mL anhydrous THF and cooled to 0 °C, and 522 mg (3.12 mmol) of LiHMDS, dissolved in 1 mL anhydrous THF, were added together followed by stirring at room temperature for 5 minutes.

This resulting solution was added dropwise to liquid sodium/NH_3 at −62 °C, and the reaction was stirred at −62 °C for 1 hour. The reaction was quenched by the addition of saturated NH_4Cl solution, NH_3 was evaporated overnight, the residue left behind was purified by dialysis (3 water changes, 16 hours) and concentrated by lyophilization to obtain 0.2 g (51%) of white fluffy gluPAS-12. ^{1}H NMR and GPC data matched those previously reported.

General procedure for sulfation. The debenzylated PASs (50 mg) and varying equivalents of $SO_3 \cdot NMe_3$ (5 eq. for glusulPAS-HS and 3 eq. for glusulPAS-LS) were suspended in 8 mL anhydrous DMF and the reaction was stirred at 50 °C for 5 days. After 5 days, the reaction was quenched by 1 M NaOH, dialyzed against DI water for 12 hours (3 water changes) and lyophilized to obtain a white fluffy solid. The residual NMe_3 in the polymer was removed by dissolving the polymer in 1 M NaOH and applying high-vacuum for 3 hours. The solution was neutralized, dialyzed (12 hours, 3 water changes) and lyophilized to obtain white, fluffy sulPAS (49 mg, 70%). The sulPASs were analyzed using SEC, ^{1}H NMR, HSQCAD, IR and CHNS analysis. Peaks in ^{1}H NMR spectra of sulfated polymers were broad and overlapping. Hence the peaks could not be assigned. HSQCAD was used instead of ^{13}C NMR as ^{13}C polymer peaks were not visible. CH_3 and CH peaks are in red and CH_2 peaks are in blue in HSQCAD spectra.

Biological assays

***Ex vivo* APTT and PT assays.**[46] 50 μL of APTT-XL reagent was added to a mixture of NHP (50 μL) and the analyte (25 μL of varying concentrations in HBS), pre-incubated at 37 °C for 5 minutes. After incubation of this mixture at 37 °C for 3 minutes, 25 μL of 0.04 M $CaCl_2$ solution was added to induce clotting. Absorbance of all the samples at 405 nm was measured every 7 seconds for a total time of upto 90 minutes. As clotting occurs, the absorbance value increases. APTT was calculated as the time taken for the absorption to increase by half the maximum value using GraphPad Prism 8.0 (GraphPad Software, San Diego, CA, USA). 25 μL of 1 IU mL^{-1} heparin solution was used as positive control. HBS was used as negative control. $CaCl_2$ in PT reagent was removed using reported procedure[46] and the prothrombin time was evaluated by the above-mentioned procedure.

A standard curve was plotted by estimating the clotting time of NHP in the presence of varying concentration of heparin (0.2–2.5 IU mL^{-1}) and fitted to exponential growth model. The anticoagulant activity of each sulPAS concentrations in IU was calculated using the equation of the curve. By dividing the activity thus obtained with the concentration used, the activity in IU mg^{-1} was calculated (Table S2†).

FXIa amidolytic activity inhibition assay. 20 μL of varying concentration of glu-50-HS was prepared and made up to 60 μL by buffer. 20 μL of FXIa (2.5 μg mL^{-1}) was added to the solution and incubated at 37 °C for 5 min. Then 20 μL of S-2366 (250 μM) was added and the absorbance at 405 nm was measured every 60 seconds. The percent inhibition of FXIa was calculated using the equation:

$$\%\ \text{inhibition} = \frac{A_0 - A_i}{A_0 - A_b} \times 100$$

where A_i is the slope of absorbance at 405 nm *vs.* time for varying concentration of analyte, A_0 is the slope in the absence of any inhibitor (positive control), A_b is the slope when FXIa was completely inhibited by adding 10 μL of 20% acetic acid before addition of the substrate (negative control).

Reversal of anticoagulant activity of sulPAS by protamine sulfate. APTT assay was repeated with 12.5 μL of glu-50-HS (200 μg mL^{-1}) and 12.5 μL of varying concentrations (25–200 μg mL^{-1}) of protamine sulfate (PS) instead of 25 μL analyte. The concentration of PS required to bring the APTT down to negative control was estimated.

Evaluation of degradation of glusulPAS by heparanase.[52] Heparin (300 μg for each trial) and glu-25-HS (300 μg for each trial) were incubated (24 h, 37 °C) with or without ($n = 3$ each) Recombinant Human Active Heparanase/HPSE protein, CF (550 ng for each trial) in a final volume of 200 μL reaction solution (0.15 M NaCl, 20 mM phosphate–citrate buffer, pH 5.8, 1 mM dithiothreitol (DTT), 1 mM $CaCl_2$). After 24 hours, the samples were lyophilized, re-dissolved in SEC buffer and retention times were evaluated.

***In vivo* coagulation assay.** Three minutes after intravenous administration of PBS, heparin or glu-50-HS, mouse blood samples were collected in citrate *via* cardiac puncture. Plasma was isolated by centrifugation at 900*g* for five minutes at room temperature. The APTT was determined using STArt microcoagulometer (Diagnostica Stago Inc., Parsippany, New Jersey) per manufacturer's instructions. Briefly, 50 μL APTT assay reagent and 50 μL plasma were incubated for 3 minutes at 37 °C. Then 50 μL pre-warmed 0.25 M $CaCl_2$ was added and clotting time was recorded in seconds. Samples that had not clotted by 999 seconds, the maximum upper threshold of the microcoagulometer, were recorded as 999 seconds.

Bleeding time. Bleeding time was evaluated by a tail vein bleeding assay, as previously described.[58] Briefly, C57BL/6 mice were anesthetized *via* intraperitoneal ketamine injection. Three minutes after intravenous administration of each agent, the tail vein was transected 10 mm from its tip and immediately submersed vertically in 50 mL warm saline (37 °C). Bleeding time was defined as time elapsed until cessation of bleeding for 30 seconds after injury.

Data availability

The raw data required to reproduce these findings are available to upon request from the authors. The processed data required to reproduce these findings are available to download from the ESI.†

Author contributions

M. V. wrote the manuscript, performed all synthetic procedures, performed chemical characterization, was involved in data collection for Fig. 2, 3, S1–S29, S31 and Tables 1, S1–S4† and prepared all figures. S. L. C. with input from R. X. performed

data collection for Fig. S30.† C. H., R. R., J. C. and E. D., performed data collection for Fig. 4 and R. R. helped edit the manuscript. E. C. and M. W. G. provided research direction, mentorship, and editing of the manuscript.

Conflicts of interest

There are no conflicts to declare.

Acknowledgements

We thank Hannah Caputo and Dr Anant S. Balijepalli for discussions in synthesis and Dr C. James McKnight of the BU School of Medicine for help in obtaining HSQCAD spectra. This work was supported in part by Boston University, DoD Uniformed Services University (HU0001810012), NIH 5T32HL007734 fellowship funding to Rae Rokosh, and Beth Israel Deaconess Medical Center.

Notes and references

1 M. B. Gorbet and M. V. Sefton, *Biomaterials*, 2004, **25**, 5681–5703.
2 W. Geerts and R. Selby, *Chest*, 2003, **124**, 357S–363S.
3 H. Chu, N. R. Johnson, N. S. Mason and Y. Wang, *J. Controlled Release*, 2011, **150**, 157–163.
4 M. F. Maitz, U. Freudenberg, M. V. Tsurkan, M. Fischer, T. Beyrich and C. Werner, *Nat. Commun.*, 2013, **4**, 1–7.
5 E. Vilanova, A. M. F. Tovar and P. A. S. Mourão, *J. Thromb. Haemostasis*, 2019, **17**, 254–256.
6 J. Fareed, W. Jeske and E. Ramacciotti, *Clin. Appl. Thromb./Hemostasis*, 2019, **25**, 1–3.
7 J. Gale, *Deadly Pig Disease Sparks Fear of Heart Drug Shortage: QuickTake – Bloomberg*, https://www.bloomberg.com/news/articles/2019-11-11/deadly-pig-disease-sparks-fear-of-heart-drug-shortage-quicktake, accessed 19 February, 2020.
8 H. Liu, Z. Zhang and R. J. Linhardt, *Nat. Prod. Rep.*, 2009, **26**, 313–321.
9 K. Hedlund, D. Coyne, D. Sanford and J. Huddelson, *Perfusion*, 2013, **28**, 61–65.
10 R. L. Bick, E. P. Frenkel, J. Walenga, J. Fareed and D. A. Hoppensteadt, *Hematology/Oncology Clinics of North America*, 2005, **19**, 1–51.
11 R. D. Rosenberg and L. Lam, *Proc. Natl. Acad. Sci. U. S. A.*, 1979, **76**, 1218–1222.
12 C. Kearon, *Chest*, 2003, **124**, 386S–392S.
13 H. Bussey, J. L. Francis and T. H. Consensus Group, *Pharmacotherapy*, 2004, **24**, 103S–107S.
14 C. Kroon, W. R. ten Hove, A. de Boer, J. M. Kroon, J. M. van der Pol, E. J. Harthoorn-Lasthuizen, H. C. Schoemaker, F. J. van der Meer and A. F. Cohen, *Circulation*, 1992, **86**, 1370–1375.
15 L. Manson, J. I. Weitz, T. J. Podor, J. Hirsh and E. Young, *J. Lab. Clin. Med.*, 1997, **130**, 649–655.
16 J. Dawes, *Acta Chir. Scand.*, 1990, 68–74.
17 T. E. Warkentin, M. N. Levine, J. Hirsh, P. Horsewood, M. K. Gent and J. G. Kelton, *N. Engl. J. Med.*, 1995, **332**, 1330–1335.
18 M. Hussain, H. P. Wendel and F. K. Gehring, *International Journal of Blood Disorders & Diseases*, 2017, **1**, 7–9.
19 T. E. Warkentin, J. A. Sheppard, P. Horsewood, P. J. Simpson, J. C. Moore and J. G. Kelton, *Blood*, 2000, **96**, 1703–1708.
20 M. Alquwaizani, L. Buckley, C. Adams and J. Fanikos, *Curr. Emerg. Hosp. Med. Rep.*, 2013, **1**, 83–97.
21 M. Wolzt, A. Weltermann, M. Nieszpaurlos, B. Schneider, A. Fassslt, K. Lechner, H. G. Eichler and P. A. Kyrle, *Thromb. Haemostasis*, 1995, **73**, 439–443.
22 K. A. Bauer, D. W. Hawkins, P. C. Peters, M. Petitou, J. M. Herbert, A. A. Van Boeckel and D. G. Meuleman, *Cardiovasc. Drug Rev.*, 2002, **20**, 37–52.
23 T. E. Warkentin, *Expert Rev. Hematol.*, 2010, **3**, 567–581.
24 A. Greinacher, T. Thiele and K. Selleng, *Thromb. Haemostasis*, 2015, **113**, 931–942.
25 C. H. Chang, L. S. Lico, T. Y. Huang, S. Y. Lin, C. L. Chang, S. D. Arco and S. C. Hung, *Angew. Chem., Int. Ed.*, 2014, **53**, 9876–9879.
26 S. J. Paluck, T. H. Nguyen and H. D. Maynard, *Biomacromolecules*, 2016, **17**, 3417–3440.
27 S. Charef, E. Petit, D. Barritault, J. Courty and J.-P. Caruelle, *J. Biomed. Mater. Res., Part A*, 2007, **83**, 1024–1031.
28 R. J. C. Fonseca and P. A. S. Mourão, *Thromb. Haemostasis*, 2006, **96**, 822–829.
29 M. Akashi, N. Sakamoto, K. Suzuki and A. Kishida, *Bioconjugate Chem.*, 1996, **7**, 393–395.
30 Y. I. Oh, G. J. Sheng, S. K. Chang and L. C. Hsieh-Wilson, *Angew. Chem., Int. Ed.*, 2013, **52**, 11796–11799.
31 D. Grande, S. Baskaran, C. Baskaran, Y. Gnanou and E. L. Chaikof, *Macromolecules*, 2000, **33**, 1123–1125.
32 Y. Huang, L. Taylor, X. Chen and N. Ayres, *J. Polym. Sci., Part A: Polym. Chem.*, 2013, **51**, 5230–5238.
33 H. Türk, R. Haag and S. Alban, *Bioconjugate Chem.*, 2004, **15**, 162–167.
34 M. Lima, T. Rudd and E. Yates, *Molecules*, 2017, **22**, 1–11.
35 J. E. Turnbull and J. T. Gallagher, *Biochem. J.*, 1991, **273**(Pt 3), 553–559.
36 M. Metzke, N. O'Connor, S. Maiti, E. Nelson and Z. Guan, *Angew. Chem., Int. Ed.*, 2005, **44**, 6529–6533.
37 L. Li, E. A. Franckowiak, Y. Xu, E. McClain and W. Du, *J. Polym. Sci., Part A: Polym. Chem.*, 2013, **51**, 3693–3699.
38 E. L. Dane and M. W. Grinstaff, *J. Am. Chem. Soc.*, 2012, **134**, 16255–16264.
39 E. L. Dane, S. L. Chin and M. W. Grinstaff, *ACS Macro Lett.*, 2013, **2**, 887–890.
40 S. E. Stidham, S. L. Chin, E. L. Dane and M. W. Grinstaff, *J. Am. Chem. Soc.*, 2014, **136**, 9544–9547.
41 S. L. Chin, Q. Lu, E. L. Dane, L. Dominguez, C. J. McKnight, J. E. Straub and M. W. Grinstaff, *J. Am. Chem. Soc.*, 2016, **138**, 6532–6540.
42 I. Capila and R. J. Linhardt, *Angew. Chem., Int. Ed.*, 2002, **41**, 391–412.
43 Y. Suhara, M. Ichikawa, J. E. K. Hildreth and Y. Ichikawa, *Tetrahedron Lett.*, 1996, **37**, 2549–2552.

44 E. S. P. Bouvier and S. M. Koza, *TrAC, Trends Anal. Chem.*, 2014, **63**, 85–94.
45 V. Kumar, A. K. Abbas and J. C. Aster, in *Robbins Basic Pathology*, 2013.
46 D. Tilley, I. Levit and J. A. Samis, *J. Visualized Exp.*, 2012, 1–7.
47 G. M. Oosta, W. T. Gardner, D. L. Beeler and R. D. Rosenberg, *Proc. Natl. Acad. Sci. U. S. A.*, 1981, **78**, 829–833.
48 W. A. Schumacher, J. M. Luettgen, M. L. Quan and D. A. Seiffert, *Arterioscler., Thromb., Vasc. Biol.*, 2010, **30**, 388–392.
49 M. L. Quan, D. J. P. Pinto, J. M. Smallheer, W. R. Ewing, K. A. Rossi, J. M. Luettgen, D. A. Seiffert and R. R. Wexler, *J. Med. Chem.*, 2018, **61**, 7425–7447.
50 M. Larsson, V. Rayzman, M. W. Nolte, K. F. Nickel, J. Björkqvist, A. Jämsä, M. P. Hardy, M. Fries, S. Schmidbauer, P. Hedenqvist, M. Broomé, I. Pragst, G. Dickneite, M. J. Wilson, A. D. Nash, C. Panousis and T. Renné, *Sci. Transl. Med.*, 2014, **6**, 1–11.
51 W. A. Wuillemin, E. Eldering, F. Citarella, C. P. De Ruig, H. Ten Cate and C. Erik Hack, *J. Biol. Chem.*, 1996, **271**, 12913–12918.
52 N. J. Nasser, G. Sarig, B. Brenner, E. Nevo, O. Goldshmidt, E. Zcharia, J. P. Li and I. Vlodavsky, *J. Thromb. Haemostasis*, 2006, **4**, 560–565.
53 G. Arturson and G. Wallenius, *Scand. J. Clin. Lab. Invest.*, 1964, **16**, 81–86.
54 T. F. Kresowik, T. W. Wakefield, R. D. Fessler 2nd and J. C. Stanley, *J. Surg. Res.*, 1988, **45**, 8–14.
55 M. Suflita, L. Fu, W. He, M. Koffas and R. J. Linhardt, *Appl. Microbiol. Biotechnol.*, 2015, **99**, 7465–7479.
56 J. A. Englaender, Y. Zhu, A. N. Shirke, L. Lin, X. Liu, F. Zhang, R. A. Gross, M. A. G. Koffas and R. J. Linhardt, *Appl. Microbiol. Biotechnol.*, 2017, **101**, 2843–2851.
57 E. L. Dane and M. W. Grinstaff, *J. Am. Chem. Soc.*, 2012, **134**, 16255–16264.
58 D. Hanjaya-Putra, C. Haller, X. Wang, E. Dai, B. Lim, L. Liu, P. Jaminet, J. Yao, A. Searle, T. Bonnard, C. E. Hagemeyer, K. Peter and E. L. Chaikof, *JCI Insight*, 2018, **3**, 1–18.